Hierarchical model for the multifractality of diffusion-limited aggregation

Jysoo Lee
Center for Polymer Studies and Department of Physics, Boston University, Boston, Massachusetts 02215

Shlomo Havlin
Center for Polymer Studies and Department of Physics, Boston University, Boston, Massachusetts 02215 and Physical Science Laboratory, DCRT, National Institutes of Health, Bethesda, Maryland 20892

H. Eugene Stanley
Center for Polymer Studies and Department of Physics, Boston University, Boston, Massachusetts 02215

James E. Kiefer
Physical Science Laboratory, DCRT, National Institutes of Health, Bethesda, Maryland 20892
(Received 28 March 1990; revised manuscript received 29 June 1990)

We propose a deterministic model of diffusion-limited aggregation (DLA), based on the concept of an *infinite hierarchy* of voids connected by narrow channels. This hierarchical model reproduces many features of DLA: (1) The growth-site probability distribution shows multifractal behavior, (2) the minimum growth probability decreases with size L as $\ln p_{\min}(L) \sim -(\ln L)^2$, and (3) the maximum growth probability scales as $p_{\max}(L) \sim L^{-\alpha_{\min}}$.

Diffusion-limited aggregation[1] (DLA) has become important for describing a wealth of diverse physical, chemical, and biological phenomena.[2] Despite many ingenious attempts,[2,3] no completely satisfactory understanding of DLA has emerged. For example, although there exist already many models of DLA structure, only the recent paper of Mandelbrot and Vicsek[4] qualitatively predicts the multifractality of the growth-site probability distribution (GSPD) and the behavior of the minimum growth probability, but the latter prediction seems to disagree with recent simulations.[5] Here we propose a hierarchical model of DLA which can be solved analytically for the GSPD and for the minimum growth probability; we shall see that all the predictions of the hierarchical model are in accord with recent simulations of DLA.

To define the model, we begin with a triangle, two sides of which have length L [Fig. 1(a)]. In the first generation of this model, we replace this triangle with the generator [Fig. 1(b)] of edge L. The generator consists of n nested subtriangles with edges $L_1, L_2, \ldots, L_n$. The edge of the largest subtriangle L_1 is aL, that of the next largest L_2 is a^2L. We continue this process until we are at the level of an individual pixel, so that the number of triangles n is fixed by the equation $L_n = a^n L = 1$ (we call this the *minimum size restriction*).[6] Therefore the maximum value of n is $-\ln L/\ln a$.

Since the total edge of the generator is the sum of edges of all the subtriangles,

$$L = \sum_{i=1}^{n} L_i = aL\frac{1-a^n}{1-a} . \tag{1}$$

For $n \gg 1$, $L \approx aL/(1-a)$; hence we choose a to be $\frac{1}{2}$.

The *second* generation[7] [Fig. 1(c)] is obtained by replacing all the subtriangles in the *first* generation with generators of edges $L/2, L/2^2, \ldots, L/2^n$ with the minimum size restriction. Third and higher generations are obtained by the analogous construction, and we continue to form higher and higher generations until we reach a "final stage" for which the edge of the largest triangle becomes 1 [Fig. 1(d)]. The concept of open voids connected by narrow channels derived direct support from visual examination of DLA clusters (cf. Fig. 2). In examining photographs of DLA from the perspective of identifying voids and channels, one must focus on that portion of DLA that is *finished* growing; Coniglio and co-workers[8] found that a large fraction of DLA is still growing (roughly the region with $r > R_g$, where R_g is the radius of gyration).

To study the fractal and multifractal[9] properties of this hierarchical model, we place the vertex O at the origin and release a random walker at the perimeter of an infinitely large circle. If the random walker touches a perimeter site of the triangle, it sticks to that site. We want to calculate the probability p_i (termed the *growth probability*) that the random walker sticks to the perimeter site i.

We will first present an analytic approach for calculating p_i, and then we check the results of the argument by direct numerical simulation. We introduce the following notation. Let the index i_1 label the voids present in the first generation [Fig. 1(b)], so that $i_1 = 1$ denotes the largest void, $i_1 = 2$ the second largest, and so on until $i_1 = n$ denotes the smallest void. Note that $n = \ln L/\ln 2$, since the edge of the smallest subtriangle is 1. For the voids created in the second generation [Fig. 1(c)], we require two indices i_1 and i_2. The maximum of i_2 is $n - i_1$, due to the minimum size restriction. For the voids created in generation q, we require q indices $(i_1, i_2, \ldots, i_q)$. Now the maximum of i_q is $n - i_1 - i_2 - \cdots - i_{q-1}$. This itera-

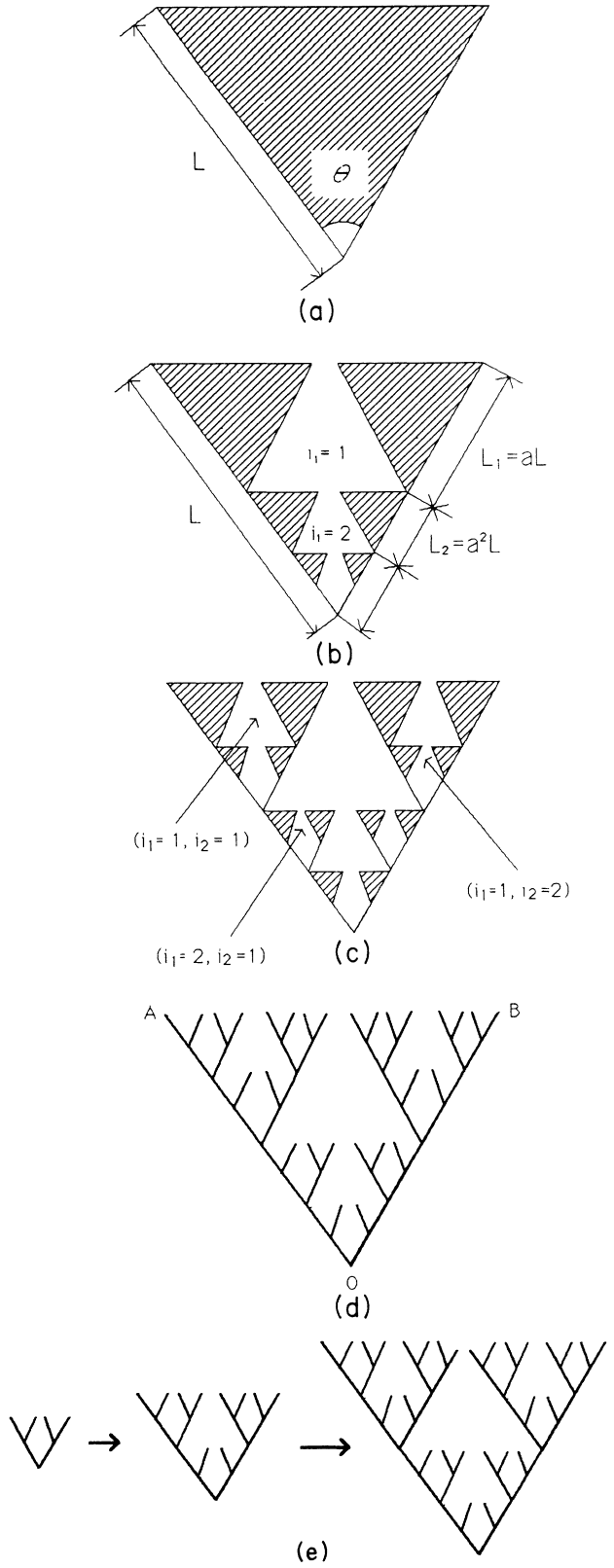

FIG. 1. A solid triangle with angle θ and side L, (b) the generator of the present hierarchical model, (c) the second generation this model, and (d) the final stage. The final stage can be generated in a simpler fashion using the construction shown in (e). However, in the text we used a more complicated generator, which is more appropriate for the analytic derivation presented.

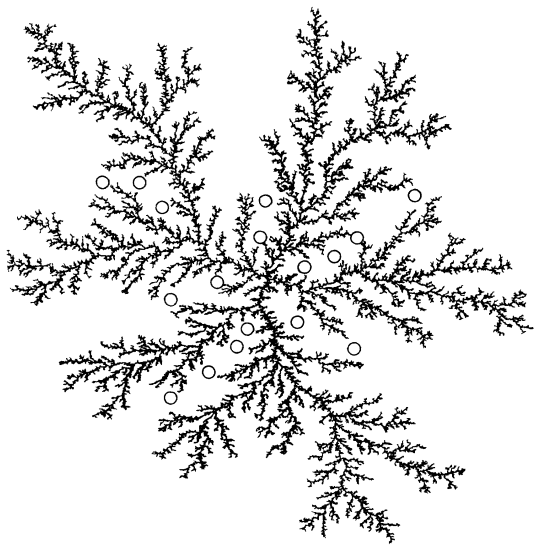

FIG. 2. Off-lattice DLA cluster of mass 100 000 (courtesy of Meakin). Indicated by small circles are some of the key channels through which a random walker must pass in order to reach the set of perimeter sites in the deepest "fjords" (it is among such sites that the quantity $p_{\min}$ will be found).

tion will terminate when all the triangles become of edge 1, which will occur after n generations. To see this, we note that in generation q, the edge of the largest triangle is $L/2^q = 2^n/2^q = 2^{n-q}$, which becomes 1 when $q = n$.

To estimate growth probabilities for the voids created in the first generation, consider again Fig. 1(b). In order for a random walker to reach the bottom of void i_1, it must pass through i_1 voids. The probability $\Pi(L)$ of passing voids of edge L scales as $\Pi(L) \sim L^{-\gamma}$.[10] Therefore the probability to reach the bottom of void i_1 is the product of the probabilities to pass through all i_1 voids,

$$p_{i_1}(L) = p_0 L_1^{-\gamma} L_2^{-\gamma} \cdots L_{i_1}^{-\gamma}$$
$$= p_0 (L/2)^{-\gamma} (L/2^2)^{-\gamma} \cdots (L/2^{i_1})^{-\gamma} . \quad (2)$$

Here p_0 is the probability to reach the entrance of the void $i_1 = 1$. Therefore the growth probability in the void i_1 is

$$p_{i_1}(L) = p_0 L^{-\gamma i_1} 2^{\gamma i_1 (i_1+1)/2} . \quad (3)$$

One can also calculate the distance of void i_1 from the vertex O, projected along the side OA (or OB). As shown in Fig. 1(b), the largest void lies between $L/2$ and L, the second largest lies between $L/4$ and $L/2$. In general,

$$2^{-i_1} < \frac{r(i_1)}{L} < 2^{-i_1+1} , \quad (4)$$

where $r(i_1)$ is the distance between a point in void i_1 and the vertex O (along the side OA).

Having obtained the growth probabilities for the voids created in generation 1, we now proceed to consider a void created in the generation q. We now label each void by q indices $(i_1, i_2, \ldots, i_q)$. For example, in Fig. 1(c) the generation $q = 2$ is shown and the new voids are

represented by the set (i_1,i_2). In order for a random walker to reach this void, it must pass through a specific sequence of other voids. Specifically, it must first reach void (i_1-1), then proceed to void (i_1,i_2-1), to (i_1,i_2,i_3-1), and so on until it finally reaches void $(i_1,i_2,\ldots,i_q)$. Therefore the growth probability $p_{i_1,i_2,\ldots,i_q}(L)$ for this void is

$$\begin{aligned} p_{i_1,i_2,\ldots,i_q}(L)=&p_{i_1-1}(L)\Pi[(i_1-1)\rightarrow(i_1,i_2-1)] \\ &\times\Pi[(i_1,i_2-1)\rightarrow(i_1,i_2,i_3-1)]\times\cdots \\ &\times\Pi[(i_1,i_2,\ldots,i_{q-1}-1) \\ &\rightarrow(i_1,i_2,\ldots,i_q)] . \end{aligned} \tag{5}$$

Here $\Pi[x\rightarrow y]$ is the probability to reach void y for the random walker starting at void x, which is obtained by noting that the transition probability $\Pi[(i_1-1)\rightarrow(i_1,i_2-1)]$ is the probability to pass through the sequence of voids $(i_1,1)\rightarrow(i_1,2)\rightarrow(i_1,3)\rightarrow\ldots\rightarrow(i_1,i_2-1)$. Since the edge of the void (i_1,i_2) is $L/2^{i_1+i_2}$,

$$\begin{aligned} &\Pi[(i_1-1)\rightarrow(i_1,i_2-1)] \\ &\quad=(L/2^{i_1+1})^{-\gamma}(L/2^{i_1+2})^{-\gamma}\ldots(L/2^{i_1+i_2-1})^{-\gamma} \\ &\quad=(L/2^{i_1})^{-\gamma(i_2-1)}2^{\gamma i_2(i_2-1)/2} . \end{aligned} \tag{6}$$

Similarly, since the edge of the void $(i_1,i_2,\ldots,i_p)$ is $L/2^{i_1+i_2+\cdots+i_p}$,

$$\begin{aligned} &\Pi[(i_1,i_2,\ldots,i_{p-1}-1)\rightarrow(i_1,i_2,\ldots,i_p-1)] \\ &\quad=(L/2^{i_1+i_2+\cdots+i_{p-1}+1})^{-\gamma}(L/2^{i_1+i_2+\cdots+ip_{p-1}+2})^{-\gamma}\cdots(L/2^{i_1+i_2+\cdots+i_{p-1}+i_q-1})^{-\gamma} \\ &\quad=(L/2^{i_1+i_2+\cdots+i_{p-1}})^{-\gamma(i_p-1)}2^{\gamma i_p(i_p-1)/2} . \end{aligned} \tag{7}$$

Substituting (7) into (5), we find

$$\begin{aligned} p_{i_1,i_2,\ldots,i_q}(L)=&L^{-\gamma(i_1-1)}2^{\gamma i_1(i_1-1)/2}(L/2^{i_1})^{-\gamma(i_2-1)}2^{\gamma i_2(i_2-1)/2} \\ &\times(L/2^{i_1+i_2})^{-\gamma(i_3-1)}2^{\gamma i_3(i_3-1)/2}\cdots(L/2^{i_1+i_2+\cdots+i_{q-1}})^{-\gamma i_q}2^{\gamma i_q(i_q+1)/2} \\ =&L^{-\gamma(i_1+i_2+\cdots+i_q-q+1)}2^{\gamma[i_1(i_2-1)+(i_1+i_2)(i_3-1)+(i_1+i_2+i_3)(i_4-1)+\cdots+(i_1+i_2+\cdots+i_{q-1})i_q]} \\ &\times2^{\gamma[i_1(i_1-1)+i_2(i_2-1)+\cdots+i_q(i_q+1)]/2} . \end{aligned} \tag{8}$$

We can also calculate the distance of void $(i_1,i_2,\ldots,i_q)$ [projected on the OA (or OB) side] from the vertex O. We already obtained this distance for $q=1$, which is (4). From Fig. 1(c), we find for general q the result

$$\begin{aligned} &2^{-i_1}+2^{-i_1-i_2}+\cdots+2^{-i_1-i_2-\cdots i_{q-1}} \\ &\quad<\frac{r(i_1,i_2,i_3,\ldots,i_q)}{L} \\ &\quad<2^{-i_1}+2^{-i_1-i_2}+\cdots+2^{-i_1-i_2-\cdots i_q} . \end{aligned} \tag{9}$$

Next we join together several hierarchical structures to form a pattern that has some similarity to DLA. For example, in Fig. 3, we connect five wedges (where the angle between the edges of each wedge is $\theta=2\pi/5$), since the off-lattice DLA typically has approximately five or six arms. We now want to calculate the growth probabilities for the perimeter sites. In the preceding section, we calculated the p_i *inside* the voids, but we did not consider the sites on the external perimeter. One can partition the external perimeter into two parts, "*lines*" ($AB,BC,\ldots$) and "*tips*" ($A,B,\ldots$). The growth probability along the lines was defined to be p_0, which we will determine below. The growth probabilities on the tips are obtained by using the known relation $p_{\max}(L)\sim p_0L^{-\alpha_{\min}}$, where $\alpha_{\min}\sim\pi/(\pi+\theta)$.[11] Thus we obtain all the growth probabilities in terms of p_0, and p_0 can be determined from the normalization condition $\sum_i p_i=1$.

For a given $L(=2^n)$, we numerically calculate (8) for $q=1,2,\ldots,n$. Here, one must be careful about the number of growth sites. There are 2^{q-1} voids having the same index $(i_1,i_2,\ldots,i_q)$. Furthermore, the edge of these voids is $L/2^{i_1+i_2+\cdots+i_q}$, which have $3L/2^{i_1+i_2+\cdots+i_q}$ growth sites. We consider two ways to

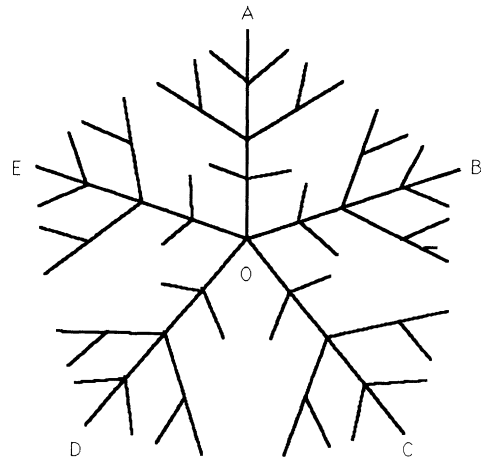

FIG. 3. Five wedges (with $\theta=2\pi/5$) connected in such a fashion to resemble DLA.

include this degeneracy. First, we consider only the growth site at the entrance to each void, ignoring all the other growth sites in the void. From these growth probabilities, we calculate the multifractal spectrum. We also calculate the multifractal spectrum as follows. Since the random walker must pass through a series of narrow channels, there may be a large difference in growth probabilities for different voids. On the other hand, there is little variation of growth probabilities inside the *same* void. Therefore we assume that all the growth sites inside the same void have the *same* growth probabilities, so we multiply the growth probability $p_{i_1,i_2,\ldots,i_q}(L)$ by a degeneracy factor $3\times 2^{n-i_1-i_2-i_3-\ldots i_q+q-1}$. We find the multifractal spectrum obtained by both of these procedures to be qualitatively similar. Therefore we present the results obtained by considering only one growth site per void.

Consider the moments of the probability distribution $\{p_i\}$,

$$Z(\beta,L)\equiv\sum_i p_i^{\beta}(L) . \tag{10a}$$

(i) First, we discuss the case $\beta>0$. Figure 4(a) is a log-log plot of $Z(\beta,L)$ versus L for $\beta=0,1,2,3,4$, with $\theta=2\pi/5$. Since we find fairly good linear behavior over two decades of L, we conclude that $Z(\beta,L)$ scales as a power law, so the exponent $F(\beta,L)$ defined by

$$Z(\beta,L)\equiv L^{-F(\beta,L)} , \tag{10b}$$

becomes independent on L for $L\gg 1$. This linear behavior is also confined by plotting successive slopes of Fig. 4(a).

(ii) Next, consider the case $\beta<0$. There are deviations from the power-law behavior, as shown in Fig. 4(b). Furthermore, the deviation becomes larger as β increases. This deviation can be understood from the fact that $p_{\min}(L)$ decays faster with L than a power law. Indeed, from Eq. (3), we obtain

$$\ln p_{\min}(L)\sim -(\ln L)^2 . \tag{11}$$

The prediction (11) of the hierarchical model is supported by recent calculations on DLA aggregates.[5] Thus the negative moments cannot scale, and there is a phase transition at $\beta_c=0$.[10,12,13]

Having established that the negative moments do not scale, we now demonstrate that the positive moments of the GSPD display multifractality. For a multifractal, $F(\beta,L)$ must be a nonlinear function of β. Since $F(\beta=1,L)=0$ by normalization, it is customary to define $D_\beta(L)$ through the relation $F(\beta,L)\equiv(\beta-1)D_\beta(L)$. Thus a test for multifractality is to see if $D_\beta(L)$ is constant: if $D_\beta(L)$ is not constant, then $F(\beta,L)$ cannot be a linear function in β. To see this, note that $D_0=d_f$, where d_f is the fractal dimension so for our model $D_0=\ln 3/\ln 2$. On the other hand, we know that $D_\infty=\alpha_{\min}$, which is $\pi/(\pi+\theta)$ $(\neq 3/\ln 2)$.

In Fig. 5(a), we also plot the numerical values of $D_\beta(L)$ for $0\le\beta\le 4$ for different values of $L(=2^n)$. One can see, especially for $0\le\beta\le 1$, the nonconstant behavior of $D_\beta(L)$. In Figs. 5(b) and 5(c), we plot $F(\beta,L)$ and its Legendre transform $S(E,L)$, respectively. Note that these multifractal spectra qualitatively resemble those found for DLA.[15]

In order to check the analytic argument presented above, we generate a hierarchical structure with $\theta=\pi/2$ [Fig. 6(a)]. For this structure, we employ the exact enumeration algorithm[14] to solve the diffusion equation in order to determine the growth probabilities and the multifractal spectrum. The free energy $F(\beta,L)$ and the entropy $S(E,L)$ obtained are shown in Figs. 6(b) and 6(c), respectively. It is seen that the difference between the analytic results of Fig. 5 and the numerical results of Fig. 6 is decreasing as the size of the system increases. For $L=64$, the difference between the analytical values of $F(\beta)$ and the numerical values is negligible. Also, the difference between the analytic and numerical values of both $E_{\min}$ and $E_{\max}$ is negligible. The difference in the fractal dimensions [determined from the maximum of the $S(E)$ function] of about 10% arises from finite-size effects. Indeed, it can be shown that both models asymptotically lead to the same values ln3/ln2.

We found that an identical hierarchical structure with

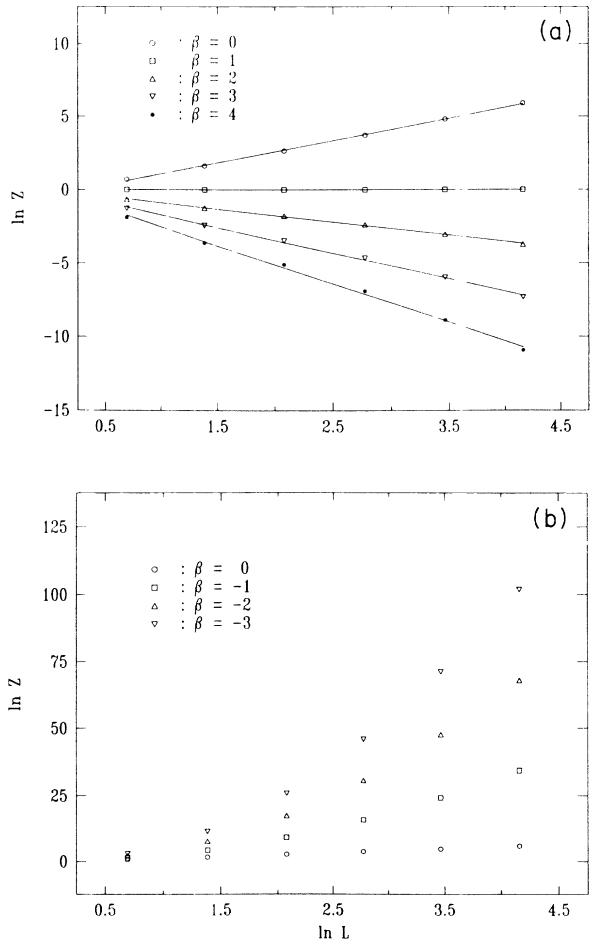

FIG. 4. Dependence of $\ln Z(\beta,L)$ on $\ln L$. (a) $\beta\ge 0$; ○, □, △, ▽, and ● denote $\beta=0$, 1, 2, 3, and 4, respectively. The data form an almost perfect straight line. (b) $\beta\le 0$; ○, □, △, and ▽ denote $\beta=0$, -1, -2, and -3, respectively. The data deviate from a straight line as β is decreased.

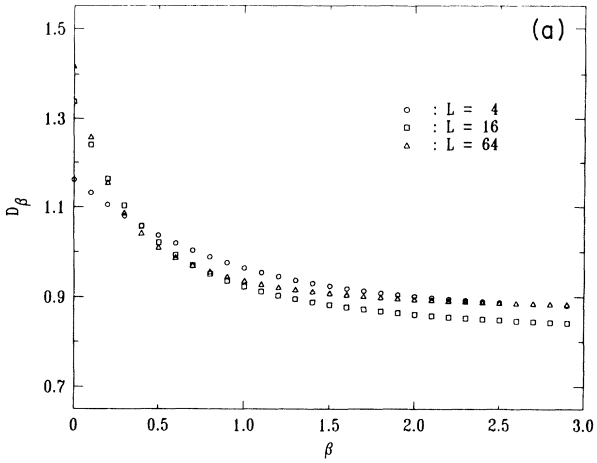

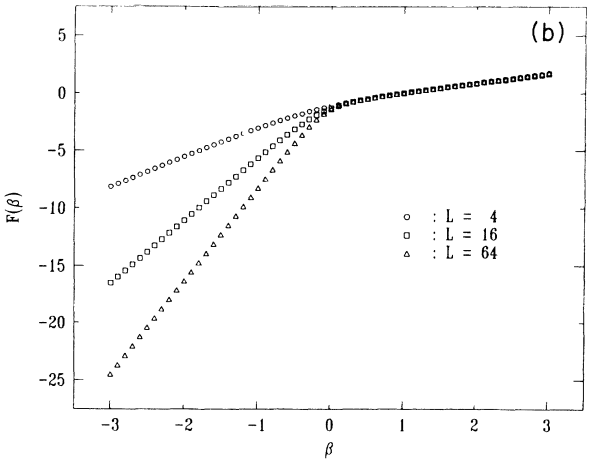

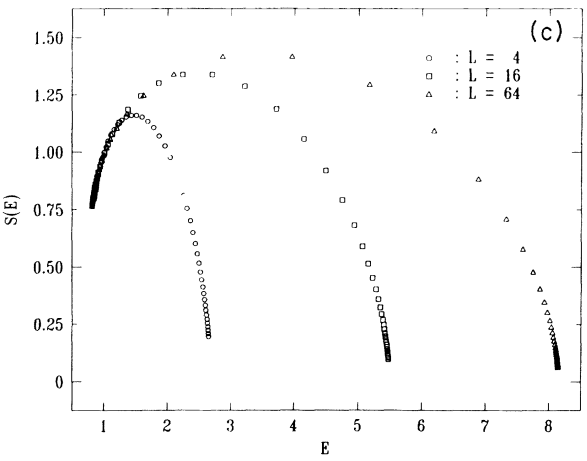

FIG. 5. (a) Plot of $D_\beta(L)$ for $0 \leq \beta \leq 4$ with different values of L. One can see a nonconstant behavior between 0 and 1. (b) Dependence of $F(\beta,L)$ on β for $L=4,16,64$. Note the good data collapse for $\beta > 0$. (c) Dependence of $S(E,L)$ on E determined for $L=4,16,64$. The left part shows good convergence. On the other hand, the right part is poorly convergent.

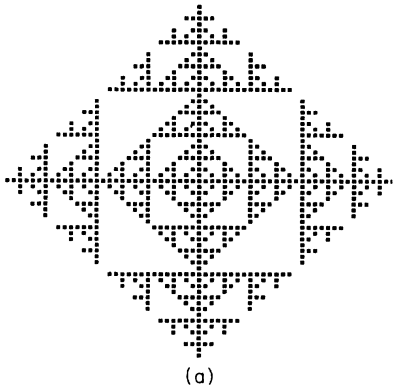

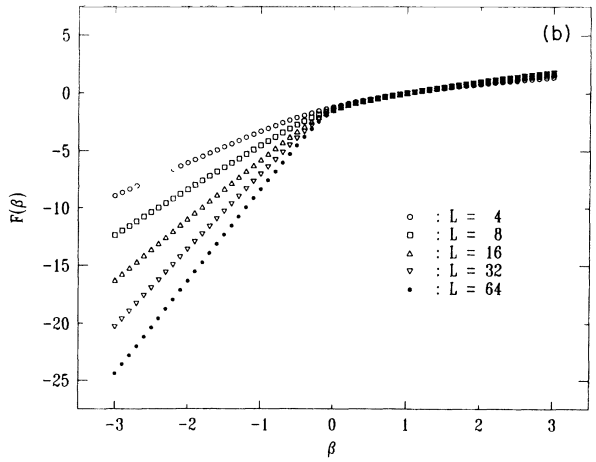

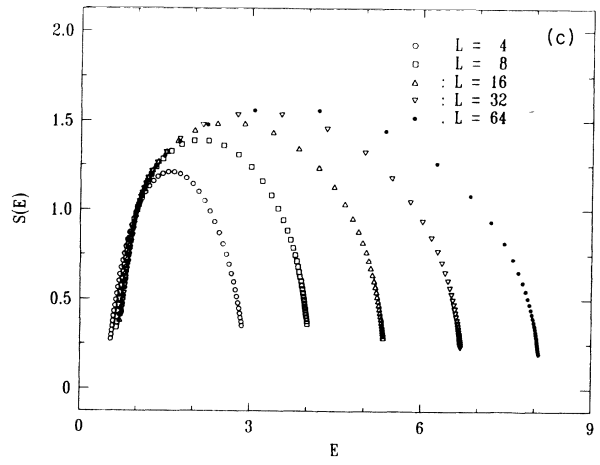

FIG. 6. (a) Clusters grown using the rule defined in the text. Note that this becomes a hierarchical structure with $\theta=\pi/2$. (b) Free energy, obtained by numerically solving the Laplace equation for $L=4,8,16,32,64$. Notice the similarity with Fig. 5(b). (c) Numerical determination of $S(E,L)$ for $L=4,8,16,32,64$. Note also the similarity with Fig. 5(c).

$\theta=\pi/2$ can be generated on the square lattice [Fig. 6(a)] by a very simple set of growth rules. Start with a seed, and at each time step check all the perimeter sites and grow the site *only if* two conditions are satisied: (i) the newly occupied site does not form a loop, and (ii) does not grow towards the origin.

We also study another quantity, the radial dependence of growth probabilities. As we see in Fig. 1(c), the largest probability $p_r(L)$ for a given distance r from the vetex O occurs in the voids from generation 1. We write Eq. (3) in a continuum form [$2^{-i_1}=r(i_1)$], and substitute into (2),

$$p_r(L)\sim p_0\exp\left[-\frac{\gamma}{\ln 2}\ln L\,\ln(r/L)\right] \quad \text{for } L\gg 1\ . \tag{12}$$

This result is supported by a numerical simulation on DLA clusters.[15]

In summary, we have developed a hierarchical model of DLA, which shows multifractality for positive β. It also predicts the "tip" behavior ($p_{\max}$ is a power law) and "fjord" behavior ($p_{\min}$ has a logarithmic singularity). The essential assumptions of this hierarchical model are (i) the diameter of the channels increase less fast with L than the diameter of the voids, and (ii) the number of voids behaves as $\ln L$.[16] Real DLA is of course random, and randomness can be incorporated in the present model by introducing randomness in the size and shape of the voids.[17]

We are grateful for discussions with A. Aharony, P. Alstrøm, A. Bunde, A. Coniglio, H. E. Roman, S. Schwarzer, D. Stauffer, and T. Vicsek, and for support from NATO, Minerva Gesellschaft für die Forschung m.b.H., the U.S. Office of Naval Research, and the National Science Foundation.

[1]T. A. Witten and L. Sander, Phys. Rev. Lett. **47**, 1400 (1981).

[2]P. Meakin, in *Phase Transitions and Critical Phenomena* edited by C. Domb and J. L. Lebowitz (Academic, Orlando, 1988), Vol. 12; J. Feder, *Fractals* (Pergamon, New York, 1988); *Random Fluctuations and Pattern Growth: Experiments and Models,* edited by H. E. Stanley and N. Ostrowsky (Kluwer Academic, Dordrecht, 1988); T. Vicsek, *Fractal Growth Phenomena* (World, Singapore, 1989); *Fractals: Physical Origin and Properties,* proceedings of the 1988 Erice Workshop on Fractals, Erice, Italy, 1988 edited by L. Pietronero (Plenum, London, 1990); *Correlations and Connectivity: Geometrical Aspects of Physics, Chemistry, and Biology,* edited by H. E. Stanley and N. Ostrowsky (Kluwer, Dordrecht, 1990), and references therein.

[3]See, e.g., L. A. Turkevich and H. Scher, Phys. Rev. Lett. **55**, 1026 (1985); R. C. Ball, R. M. Brady, G. Rossi, and B. R. Thompson, Phys. Rev. Lett. **55**, 1406 (1985); A. Coniglio, in *On Growth and Form: Fractal and Non-Fractal Patterns in Physics,* edited by H. E. Stanley and N. Ostrowsky (Nijhoff, Dordrecht, 1985), p. 101; G. Parisi and Y. C. Zhang, J. Stat. Phys. **41**, 1 (1985); Y. Hayakawa, S. Sato, and M. Matsushita, Phys. Rev. A **36**, 1963 (1987); T. C. Halsey, Phys. Rev. Lett. **59**, 2067 (1987). Recently L. Pietronero, A. Erzan, and C. Evertsz [Phys. Rev. Lett. **61**, 861 (1988)] have presented a general theory of fractal growth which includes DLA as an example.

[4]B. B. Mandelbrot and T. Vicsek, J. Phys. A **22**, L377 (1989).

[5]S. Schwarzer, J. Lee, A. Bunde, S. Havlin, H. E. Roman, and H. E. Stanley, Phys. Rev. Lett. **65**, 603 (1990). Note also that the present hierarchical model is a generalization of the model proposed by the above work, since here each solid triangle is replaced by fractal structures.

[6]Here the length scale unity is the smallest length scale we want to probe with a random walker.

[7]At this level, the present model differs from the model of Ref. 5.

[8]A. Coniglio and M. Zannetti, Physica A **163**, 325 (1990); C. Amitrano, A. Coniglio, P. Meakin, and M. Zanetti (unpublished).

[9]B. B. Mandelbrot, J. Fluid Mech. **62**, 331 (1974); *Random Fluctuations and Pattern Growth: Experiments and Models,* Ref. 3, p. 279; H. G. E. Hentschel and I. Procaccia, Physica D **8**, 435 (1983); R. Benzi, G. Paladin, G. Parisi, and A. Vulpiani, J. Phys. A **17**, 3521 (1984); T. C. Halsey, M. H. Jensen, L. P. Kadanoff, I. Procaccia, and B. I. Shraiman, Phys. Rev. A **33**, 1141 (1986). The multifractality in DLA was studied by many authors [see, e.g., C. Amitrano, A. Coniglio, and F. di Liberto, Phys. Rev. Lett. **57**, 1016 (1986)].

[10]By assuming the shape of the open space to be a triangle, one finds γ to be π/θ. See, e.g., P. Meakin, A. Coniglio, H. E. Stanley, and T. A. Witten, Phys. Rev. A **34**, 3325 (1986). For more general "lagoon" structure, Harris and Cohen [Phys. Rev. A **41**, 971 (1990)] find a similar scaling relation.

[11]The model of L. Turkevich and H. Scher (TS) [Phys. Rev. Lett. **55**, 1026 (1985)] is a special subset of the present hierarchical model, in the sense that TS focus on the wedge-shaped tips ($A,B,\ldots$), while we include the internal structure behind the tips.

[12]J. Lee and H. E. Stanley, Phys. Rev. Lett. **61**, 2945 (1988).

[13]R. Blumenfeld and A. Aharony, Phys. Rev. Lett. **62**, 2977 (1989). See also P. Trunfio and P. Alstrøm, Phys. Rev. B **41**, 896 (1990); A. B. Harris and M. Cohen, Phys. Rev. A **41**, 971 (1990); B. Fourcade and A-M. S. Tremblay, Phys. Rev. Lett. **64**, 1842 (1990).

[14]S. Havlin and B. L. Trus, J. Phys. A **21**, L731 (1988).

[15]S. Schwarzer, J. Lee, A. Bunde, S. Havlin, H. E. Roman, and H. E. Stanley (unpublished).

[16]It is not so difficult to generalize these assumptions. For example, by assuming the number of voids scales as L^x, one can show that $p_{\min}(L)\sim\exp(-L^y)$ (Ref. 15). However, we emphasize that the recent numerical simulation favors $\ln L$ behavior.

[17]For real DLA, the scaling form of the growth site probability distribution has recently been studied for clusters of size up to 20 000 sites [S. Schwarzer, J. Lee, S. Havlin, P. Meakin, and H. E. Stanley (unpublished)].